Critical appraisal on the role of catalysts for the oxygen reduction reaction in lithium-oxygen batteries

Andrew W. Lodge [a], Matthew J. Lacey [b], Matthew Fitt [a], Nuria Garcia-Araez [a,*], John R. Owen [a,*]

[a] University of Southampton, Chemistry, Southampton SO17 1BJ, United Kingdom
[b] Department of Chemistry – Ångstrom Laboratory, Uppsala University, Box 538, SE-75121 Uppsala, Sweden

ARTICLE INFO

ABSTRACT

This work reports a detailed characterization of the reduction of oxygen in pyrrolidinium-based ionic liquids for application to lithium-oxygen batteries. It is found that, in the absence of Li$^+$, all electron transfer kinetics are fast, and therefore, the reactions are limited by the mass transport rate. Reversible reduction of O_2 to $O_2^{\bullet-}$ and $O_2^{\bullet-}$ to O_2^{2-} take place at E^0 = 2.1 V and 0.8 V vs. Li$^+$/Li, respectively. In the presence of Li$^+$, O_2 is reduced to LiO_2 first and then to Li_2O_2. The solubility product constant of Li_2O_2 is found to be around 10^{-51}, corroborating the hypothesis that electrode passivation by Li_2O_2 deposition is an important issue that limits the capacity delivered by lithium-oxygen batteries. Enhancing the rate of Li_2O_2 formation by using different electrode materials would probably lead to faster electrode passivation and hence smaller charge due to oxygen reduction (smaller capacity of the battery). On the contrary, soluble redox catalysts can not only increase the reaction rate of Li_2O_2 formation but also avoid electrode passivation since the fast diffusion of the soluble redox catalyst would displace the formation of Li_2O_2 at a sufficient distance from the electrode surface.

© 2014 Published by Elsevier Ltd.

1. Introduction

It is necessary to decrease the oil dependency, not only because its consumption generates CO_2 and other pollutants, but also because its resources are limited and its price can only increase in the future. The majority of oil is used for automobile and light truck applications, and therefore the development of longer driving range electric vehicles is imperative [1,2]. Non-aqueous lithium-oxygen batteries are promising candidates to power the future electric vehicles, since they can potentially deliver a specific energy (i.e. energy per unit mass) 5 times higher than lithium-ion [3–7]. For example, a lithium-O_2 cell with a 90% porous positive electrode has a theoretical specific energy of c.a. 3000 Wh kg^{-1} (where the mass of the electrodes and the Li_2O_2 discharge product has been included in the calculation) [8]. However, the practical energy delivered by the state-of-the-art lithium-oxygen batteries is much smaller, even though these batteries are usually run at a very slow discharge rate (the full discharge of the battery may take several days) so that even very slow reactions will have enough time to proceed.

Several factors limit the performance of the state-of-the-art lithium-oxygen batteries. As described before, the power capability of the battery is very low, and this is associated with slow reaction kinetics. The capacity of the battery (i.e. charge per unit mass) is also low. This is mainly due to the passivation of the positive electrode by deposition of the discharge products, which are insoluble and insulating [9]. Additional issues are related with side reactions such as the degradation of the electrolyte [10–13], or the corrosion of the carbon-containing positive electrode [14–18].

In the absence of degradation reactions, the discharge of a lithium-oxygen battery involves the reduction of O_2 at the positive electrode to form Li_2O_2 [19,20]. In this work, a detailed study of the mechanism of O_2 reduction in 1-butyl-1-methylpyrrolidinium bis(trifluoromethylsulfonyl)imide (Pyr_{14}TFSI) (see chemical formula in Fig. 1) is reported. This ionic liquid is a promising choice of electrolyte for lithium-oxygen batteries, because it is resistant to degradation, has a wide electrochemical stability window, it is hydrophobic and is non-volatile [20–32]. Previous studies using Pyr_{14}TFSI in lithium-oxygen batteries have reported promising electrochemical performance in terms of discharge capacity at high discharge rate, cyclability and absence of degradation reactions [20,31,32]. However, further improvements in the performance of the cells are still required for practical applications, and for that purpose, it is important to identify the main factors limiting the

* Corresponding author.
E-mail addresses: n.garcia-araez@soton.ac.uk (N. Garcia-Araez),
J.R.Owen@soton.ac.uk (J.R. Owen).
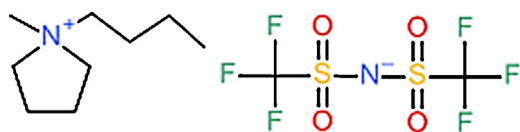
Fig. 1. The chemical formula of the ionic liquid 1-butyl-1-methylpyrrolidinium bis(trifluoromethylsulfonyl)imide ($Pyr_{14}TFSI$) used for the experiments.

performance. This work provides a detailed mechanistic study of the reduction of oxygen, first in the pure ionic liquid, and then in the presence of Li^+. The solubility product constant of the reaction product, Li_2O_2, is found to be very small: 10^{-51}. Consequently, it is concluded that electrode materials with high activity towards the reduction of oxygen will produce a faster deposition of Li_2O_2 on the electrode surface, resulting in fast electrode passivation. Therefore, less catalytic materials may produce better electrochemical performance, in terms of higher oxygen reduction charge.
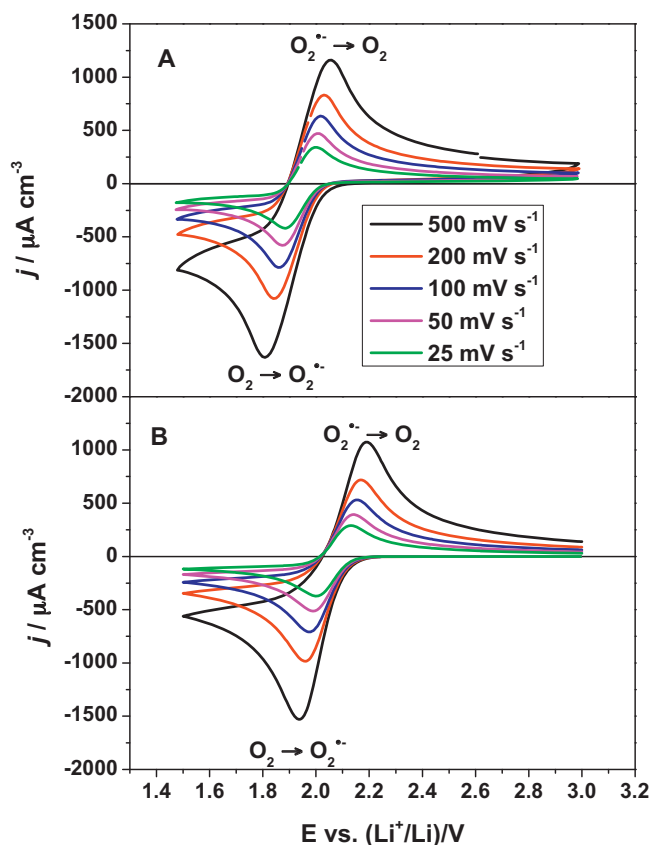
2. Experimental

1-butyl-1-methylpyrrolidinum bis(trifluoromethylsulfonyl) imide ($Pyr_{14}TFSI$) (99%, IoLiTec Ionic Liquids Technologies GmbH, Germany) and bis(trifluoromethane)-sulfonamide lithium salt (LiTFSI) (99.95%, Aldrich) were dried and deoxygenated under a vacuum at 120 °C for approximately 18 hours. The water content of the dried $Pyr_{14}TFSI$ was <10 ppm, as determined by Karl Fischer measurements [33].

The glassy carbon macrodisc electrode was constructed by sealing glassy carbon rods in glass. The platinum microdisc electrode was constructed by sealing a platinum wire (99.99%, Alfa Aesar) in glass. Prior to each experiment, the working electrodes were polished with 0.3 μm and 0.05 μm alumina powder (Buehler), and rinsed and sonicated with acetone and water. The size of the electrodes was evaluated by measuring the cyclic voltammograms in a solution of $0.01 M K_4FeCN_6 + 0.01 M K_3FeCN_6 + 0.1 M KCl$ in water. The radius of the macrodisc glassy carbon electrode was 1.5 mm and the radius of the platinum microelectrode was 13.5 μm.

The counter electrode was a platinum gauze counter electrode that was cleaned by flame annealing. For most of the experiments, a lithium foil (99.99%, Chemetall GmbH) pressed onto stainless steel gauze was used as the reference electrode. For the experiments shown in Fig. 3, a $Li_{1.5}Mn_2O_4$ spinel intercalation electrode was used as reference electrode. The $Li_{1.5}Mn_2O_4$ ink was synthesised by mixing $LiMn_2O_4$ (Carus Chemical co.) and LiI (99%, Acros Organics) in a 2:1 molar ratio and heating in a furnace at 150 °C for 24 hours. The resulting $Li_{1.5}Mn_2O_4$ powder was then added to PVDF (Solvay Solexis Ltd), carbon black (Chevron Philips Chemical Co.) and cyclopentanone (≥ 99%, Sigma-Aldrich) and the solution was heated and stirred to form an ink. A 0.5 mm diameter platinum wire was dip coated in $Li_{1.5}Mn_2O_4$ ink and left to dry. The coated wire was then placed into a fritted glass tube containing two drops of a 10 mM solution of LiTFSI in $Pyr_{14}TFSI$. This reference electrode gave a potential of +2.98 V vs. Li^+/Li. All data obtained using this electrode has been converted to the Li^+/Li scale accordingly.

Prior to each experiment, the electrodes and the glass-made electrochemical cell were dried in an oven at 80 °C overnight. The electrochemical cells were assembled inside an argon glovebox (< 1 ppm water content, < 10 ppm oxygen content). The ionic liquid was saturated with oxygen (99.5%, BOC) by bubbling through a needle into the ionic liquid for approximately 15 minutes.

Cyclic voltammetry was done using a Bio-logic VMP 2 variable multichannel potentiostat/galvanostat equipped with a low current channel, or an Iviumsoft Compactstat potentiostat. All measurements involving a microelectrode were done in an earthed Faraday cage to remove any background interference from the

Fig. 2. Experimental (A) and simulated (B) cyclic voltammograms showing the one-electron reduction of oxygen in $Pyr_{14}TFSI$ at a 3 mm diameter glassy carbon disc at different scan rates (500, 200, 100, 50 and 25 mV s^{-1}). The parameters used for the simulations are: $E^0 (O_2/O_2^{•-}) = 2.1$ V vs. Li^+/Li, $k^0 (O_2/O_2^{•-}) = 0.001$ cm s^{-1}, $D_{O_2} = 1.2 \times 10^{-5}$ cm^2 s^{-1}, $[O_2] = 3$ mM, and $D_{O_2^-} = 1 \times 10^{-6}$ cm^2 s^{-1}.

observed signal. All measurements were carried out at ambient room temperature, approximately 25 °C. Simulation of the voltammograms was done with a simulation package, DigiElch Version 7.FD, based on finite difference methods. The experimental data obtained with a macroelectrode are simulated with one-dimensional semi-infinite diffusion, and three-dimensional diffusion is used for the results with a microelectrode disk.

3. Results and discussion

3.1. Pure $Pyr_{14}TFSI$

Fig. 2A shows cyclic voltammograms of the oxygen reduction reaction on a glassy carbon macroelectrode in the pure $Pyr_{14}TFSI$ ionic liquid at different scan rates. These electrochemical measurements are very sensitive to the presence of impurities in the ionic liquids [26,34], and the characteristic shape of the voltammograms in Fig. 2A demonstrates the high purity of the materials employed here, in reasonably good agreement with previous works [22,25,26,30,31,34–40]. Simulated voltammograms, as shown in Fig. 2B, agree well with the experiments. From the comparison of the experimental data and the simulations, it can be concluded that the transfer of one electron to oxygen, forming superoxide, $O_2^{•-}$, is fast and reversible and the standard potential is around 2.1 V vs. Li^+/Li. Under the present conditions, the reaction rate is determined by the rate of diffusion of oxygen, which is can be related to the product $D_{O_2}^{1/2}[O_2]$ where D_{O_2} is the diffusion coefficient of O_2 and $[O_2]$ is the O_2 solubility. In order to determine the individual values of D_{O_2} and $[O_2]$, additional experimental data are required.